Shear Strength of Dense Sands During Rapid Loading

K.J. McManus
PhD
Senior Lecturer, Dept. of Civil Engineering, University of Canterbury, New Zealand
R.O. Davis
PhD, FIPENZ
Reader, Dept. of Civil Engineering, University of Canterbury, New Zealand

Summary Dilation during undrained shear in saturated triaxial samples of sand leads to cavitation of the pore fluid. The onset of cavitation is observed by direct measurement of pore pressure, by measurement of sample volume change, and by an abrupt change in both deviatoric stress-strain response and stress path behaviour. The implications of cavitation are significant in situations where rapid loading of dense saturated soils may occur. A simple method for predicting shear strength with cavitation is presented.

1. INTRODUCTION

The possibility of cavitation of pore fluid induced by shearing and dilation in a dense sand is of considerable importance with regard to the undrained strength of soils. During rapid deformation, such as may occur in an earthquake or any form of dynamic loading, dense sands may gain significant amounts of strength due to reduction of pore pressure caused by dilation. In general the undrained strength of a sand may be several times greater than its drained strength. However, if cavitation occurs in the pore fluid, the nature of loading will abruptly change from undrained to drained. The enhanced strength expected from undrained conditions may be only partially manifest should cavitation occur.

This paper describes an investigation of dilation induced cavitation during undrained triaxial compression tests on fully saturated samples of dense sand. The possibility of cavitation has been noted by other researchers. Whitman and Healy (1962) detected cavitation while performing rapid loading triaxial tests on sand. They inferred that cavitation had occurred in their samples because of a characteristic change in the test response from typical undrained behaviour to that typical of drained behaviour. Lee (1965), observed cavitation in a series of undrained triaxial tests on dense sand samples. He also noted that for sufficiently high values of confining stress, cavitation did not occur, there being less dilational potential as confining stress increases. Inspection of the geotechnical literature suggests that no other researchers have directly commented upon cavitation, and no one appears to have carried out tests specifically aimed at observation of cavitation effects. In what follows, we present evidence that cavitation can occur spontaneously in a saturated sand during undrained shear. We demonstrate that the response of the sand sample changes from undrained to drained at the point where measurements indicate a pore pressure of negative one atmosphere. We examine the stress path behaviour of soil undergoing cavitation and present a simple method for predicting shear strength.

2. TRIAXIAL TESTING

The tests described here were performed on 75 *mm* diameter samples of a medium silica sand with sub-angular particles having a D_{50} of 0.46 *mm* and uniformity coefficient of 1.5. Samples were prepared in a conventional split mould by tamping moist sand in layers to produce a relative density of 86 percent. The samples were saturated by first applying a high vacuum of roughly -96 *kPa* for 10 hours. Next, carbon dioxide gas was introduced twice at a pressure of 100 *kPa* then removed by vacuum, the purpose being to flush any remaining air from the sample. Then de-aired water was introduced under vacuum and flushed through the sample with backpressure increasing to 500 *kPa*. Finally the samples were consolidated with an effective confining stress of 500 *kPa*. In all tests the degree of saturation of the sample was sufficiently high to produce a *B* value of 0.98 or better.

A full complement of conventional instrumentation was used to monitor sample response. In all tests, measurements of axial force were made using an in-cell load cell to eliminate effects of plunger friction. Axial displacement was measured with a linear strain conversion transducer (LSCT). Both cell pressure and pore pressure were continuously monitored by pressure transducers. In addition, one unconventional measurement was made: the sample volume change was continuously monitored throughout each test by measuring the change of volume of the cell fluid. This was accomplished by using a double-rolling-diaphragm volume measurement cylinder and digital dial gauge and proved to be an effective and accurate way to monitor the sample volume. A simple linear correction for the change in plunger volume inside the cell, based on the measured axial displacement, was used. A correction also was made for small volume changes caused by creep of the acrylic cell while under pressure. These corrections were determined by pressurising the cell without a soil sample and measuring cell volume change with time. The rate of creep was observed to decay with time and was closely fitted by a logarithmic curve. This curve was used subsequently to make the creep corrections for all the tests. Leakage of cell fluid was not observed in any of our tests, the cell design incorporating an o-ring seal for the plunger.

Tests were performed at a constant rate of displacement of 0.5 *mm* per minute. Measurements of all channels of instrumentation were stored in a computer for subsequent inspection. One drained test was performed in order to compare the sample volume change measured directly from change in pore fluid volume with the similar measurement made by monitoring the cell fluid volume. Three undrained tests were then performed at different values of back pressure but with the same net confining stress of 50 *kPa*. Loading was continued until the axial force stabilised. The sample was then unloaded, reducing the plunger load to zero and leaving the sample in a hydrostatic state of stress.

3. RESULTS

Figure 1 shows results from the single drained test we performed. The cell confining stress for the test was 50 *kPa*. Figure 1a shows typical stress-strain response for the dense sand. Of more interest is Figure 1b in which plots of volumetric strain are shown. One of the curves on Figure 1b was made by directly measuring the volume of pore fluid moving into or out of the sample in the conventional manner. The second curve was obtained by measuring the volume of water moving into or out of the triaxial cell, corrected for the volume of the plunger and for creep effects. The two measurements agree closely over the full range of axial strain.

Results from the three undrained tests are illustrated in Figures 2 through 5. These tests were all performed with a confining stress of 50 *kPa*. They differ only in the amount of back pressure imposed initially on the sample. Back pressures of 150, 350, and 550 *kPa* were used for the three tests. Figure 2 shows graphs of stress deviator versus axial strain and gauge pore pressure versus axial strain for the tests. As these graphs make clear, the pore pressure in each test begins at the imposed back pressure value, but then decreases until cavitation occurs at a value of roughly -97 *kPa*. All three graphs have a roughly similar slope before cavitation, indicating that the dilational potential of the sand remained constant as the deviatoric stress increased. Careful inspection of the stress-strain plots in this figure also reveals a distinct change in slope of the stress-strain response for all three tests which corresponds exactly to the point at which cavitation occurred.

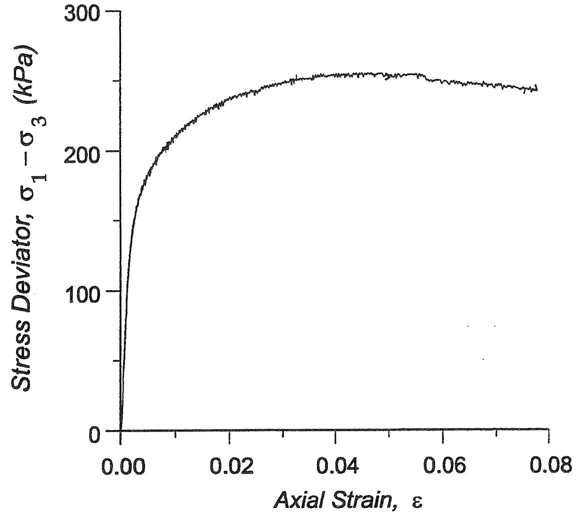

Figure 1a. Drained stress-strain response

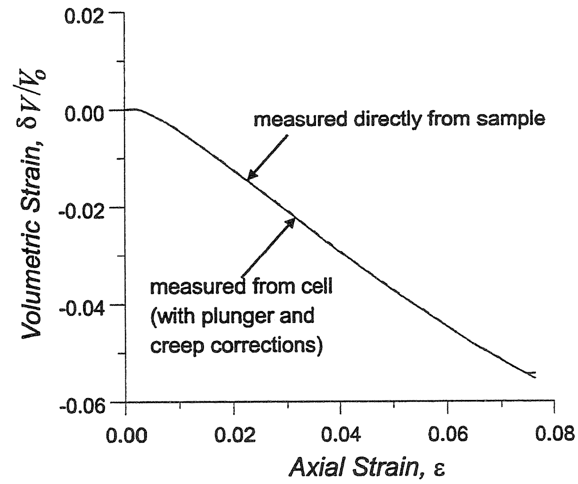

Figure 1b. Volumetric strain - axial strain response

Figure 3 shows the sample volumetric strain, measured from the volume change of cell water, plotted against axial strain. The effects of cavitation are quite clear on this figure, the sample volume remaining nearly constant before cavitation, but exhibiting dilation following cavitation. The slope of the volumetric strain-axial strain response following cavitation is similar for all three tests, although careful inspection shows a slight increase in slope (becoming less negative) as back pressure increases. This is expected since the effective confining stress for the drained (post-cavitation) response is increasing. In each test, when cavitation occurs, the effective confining stress is equal to the applied cell pressure of 200, 400, or 600 *kPa*, plus the cavitation pressure of 100 *kPa*. We expect to find that the rate of dilation is less pronounced as effective stress increases.

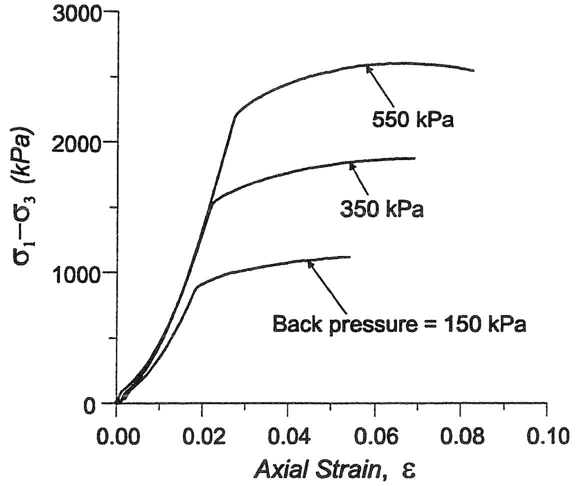

Figure 2a. Undrained stress - strain response

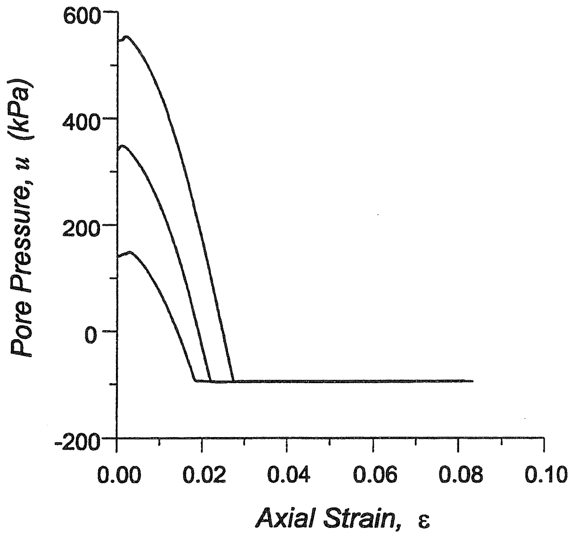

Figure 2b. Undrained pore pressure response.

Figure 4 illustrates the stress paths for the three undrained tests. Cavitation is distinctly evident here also. In each test the initial stress path is nearly the same. When cavitation occurs, the stress path slope abruptly changes to become equal to the drained value of 1.0. These changes occur at precisely the points where cavitation was measured. It is also interesting to note that if we project the drained stress path back down to the level of zero deviator stress, it intersects the mean stress axis at exactly the value of confining stress mentioned in the preceding paragraph.

Finally, in Figure 5, we illustrate the unloading response of one of the samples after cavitation had occurred. The test shown was the third of the undrained series having a back pressure of 550 *kPa*. Figure 5a shows the stress path for both the loading and unloading phases. During unloading the sample continues to behave as a drained soil, the stress path having a slope of almost exactly 1.0. The sample volumetric strain versus axial strain is shown in Figure 5b. It is clear from this figure that the sample recovers some of the dilation suffered post cavitation, but there is some permanent deformation as well. Throughout the unloading, the sample pore pressure remained constant at approximately negative one atmosphere. When the deviatoric stress had been reduced to zero, the sample was in a hydrostatic state of stress under the combined action of the cell pressure and the negative pore pressure.

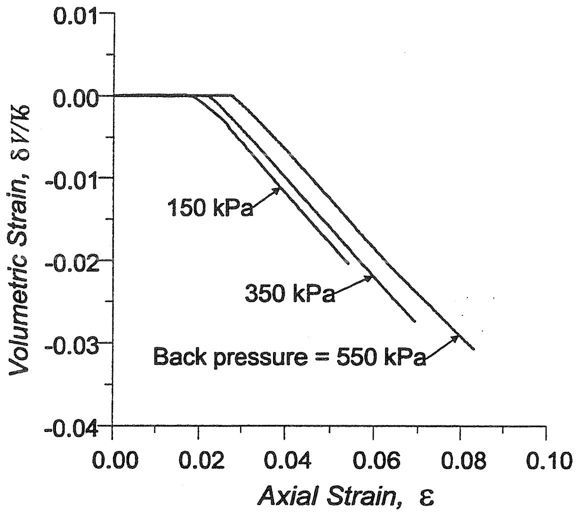

Figure 3. Undrained volumetric strain response.

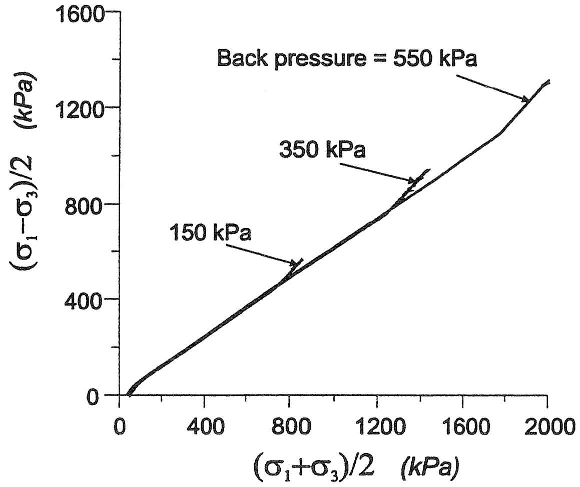

Figure 4. Undrained stress paths.

4. DISCUSSION

The results obtained here make clear that cavitation of pore fluid can occur spontaneously during shearing of dense sand. Further, it is clear that when cavitation occurs the shear strength of the soil is curtailed and may be far less than the full undrained value that might otherwise be expected. Implications of cavitation are of importance in practical situations where dynamic loads lead to rapid changes in pore pressure within a soil deposit. In this section we examine the stress path behaviour of soil undergoing cavitation and present a simple method for predicting shear strength.

The stress path behaviour observed in the tests may be explained with reference to Figure 6. The total

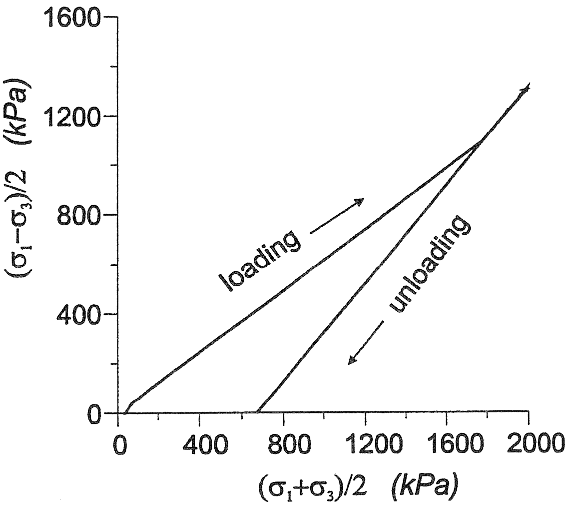

Figure 5a. Stress path for 550 kPa back pressure test.

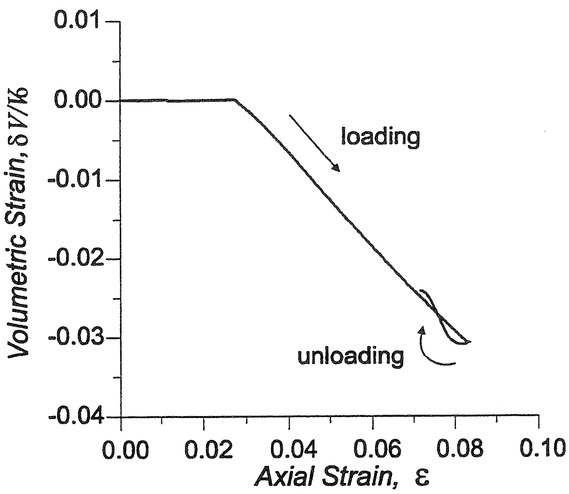

Figure 5b. Undrained volumetric strain response.

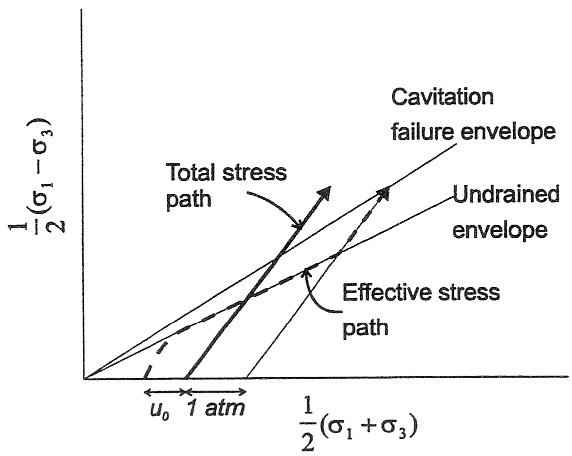

Figure 6. Predicting shear strength with cavitation.

stress path of loading is indicated as a straight line rising with positive slope. The soil average effective stress initially is reduced below the total stress by an amount equal to u_o, the initial pore water pressure. As the soil is loaded, u decreases rapidly and the effective stress path is deflected to the right and tends to follow the line we have labelled "undrained envelope". When u reduces to below 0, the effective stress path crosses to the right hand side of the total stress path, as shown. When cavitation occurs, u is constrained to a constant value of -1 atmosphere and so the effective stress path deflects upward to parallel the total stress path. The specimen fails when it reaches the line we have labelled "cavitation failure envelope". For these tests the "cavitation failure envelope" was found to have a slope of $\alpha = 29°$ equivalent to a friction angle of $\phi = 33°$. The slope of the "undrained envelope" was found to be $\alpha = 27°$, equivalent to a friction angle of 31°.

It would seem logical to predict that the "cavitation failure envelope" shown in Figure 6 should be the same as the drained failure envelope since the soil was dilating during the tests with cavitation. Only a single drained test was conducted and this reached a peak friction angle of 35°, slightly higher than the 33° reached by the cavitating specimens. However, the peak strengths of the cavitating specimens were all attained at much higher confining stresses than for the single drained test (300, 500, and 700 kPa compared to 50 kPa) and so the observed reduction in peak friction angle may be expected (e.g., Bolton, 1986).

The slope of the "undrained envelope" shown in Figure 6 should be just slightly above the steady state friction angle for the soil, as is usual for undrained triaxial testing of dense sands (e.g., Atkinson and Branby, 1978).

The shear strength of sand during rapid loading may therefore be predicted from the total stress path and the drained friction angle, ϕ. Using Figure 6 it is necessary simply to draw the drained failure envelope ($\tan \alpha = \sin \phi$) and the total stress path of loading. Then draw a line parallel to the total stress path and offset by 1 atmosphere. The point of intersection with the failure envelope gives the predicted shear strength.

5. REFERENCES

Atkinson, J.H., and Branby, P.L. (1978) *The Mechanics of Soils*, McGraw-Hill, Maidenhead, U.K., 375p.

Bolton, M.D. (1986) The Strength and Dilatancy of Sands, *Geotechnique*, 36(1), pp. 65-78.

Lee, K.L. (1965) *Triaxial Compressive Strength of Saturated Sand Under Seismic Loading Conditions*, Ph.D. Thesis, University of California, Berkeley, 521p.

Whitman, R.V., and Healy, K.A. (1962) Shear strength of sand during rapid loading, *Jour. Soil Mech. Founds. Div., ASCE*, Vol.88, SM2, pp. 99-132.